

Supporting information for

Iodine-doping sulfurized polyacrylonitrile with enhanced electrochemical
performance for room-temperature sodium/potassium sulfur batteries

Shaobo Ma^a, Pengjian Zuo^{a,*}, Han Zhang^b, Zhenjiang Yu^a, Can Cui^a, Mengxue He^a,
Geping Yin^a

a MITT Key Laboratory of Critical Materials Technology for New Energy
Conversion and Storage, School of Chemistry and Chemical Engineering, Harbin
Institute of Technology, Harbin 150001, China

b State Key Laboratory of Power Equipment & System Security and New Technology,
Chongqing University, Chongqing 400044, China

*Corresponding author

E-mail: zuopj@hit.edu.cn

Experimental section

1.1 Preparation of the I-S@pPAN cathode

0.4 g of monomer acrylonitrile (AN, Aldrich), 1.36 g of sublimed sulfur (Aladdin) and 0.24 g iodine (Aladdin) were dispersed in 10 ml ethanol medium, followed by a balling-milling process for 8 h. After centrifuged and washed with ethanol for several times, the mixture was dried at 70 °C in a vacuum oven for 24 h. Then the mixture was sealed in a quartz tube filled with argon gas and heated at 300 °C for 10 h. After cooling down, the obtained product denoted as I-S@pPAN was disposed with grinding and sieving (200 mesh). For S@pPAN synthesis by the similar procedure, the mass of monomer acrylonitrile and sublimed sulfur were 0.4 g and 1.6 g, respectively.

1.2 Alkali metal-sulfur batteries assembly and electrochemical measurements

The electrochemical performance of the samples was evaluated with CR-2025 type coin cells assembled in an argon-filled glove box. The positive electrodes were fabricated by mixing active materials, Super P and polyvinylidene fluoride (PVDF) in a weight ratio of 8:1:1. After stirring about 12 h, the homogeneous slurry was casted onto the carbon-coated aluminum foil and dried at 70 °C under vacuum overnight. The electrode film was punched into round disks with a diameter of 14 mm, and the area loading of I-S@pPAN in the electrode was around 1.0 mg cm⁻². The electrolyte/sulfur ratio is around 380 μL/mg. For the measurement of RT-Na/S and RT-K/S batteries, the kinds of electrolyte were 1 M sodium perchlorate (NaClO₄) + ethylene carbonate/ dimethyl carbonate (EC:DEC, volume ratio=1:1) + 8% fluoroethylene carbonate (FEC), 0.8 M potassium hexafluorophosphate (KPF₆) + EC/DEC (volume ratio=1:1), respectively. The Whatman glass fibres were used as separators for RT-Na/S battery (GF/D 1823) and RT-K/S battery (GF/A 1820). The galvanostatic measurement was performed at Neware Battery Testing System at 28 °C. Electrochemical impedance spectroscopy (EIS) measurements were performed on a PARSTAT 2273 workstation in the frequency range between 10⁻² and 10⁵ Hz with an amplitude of 10 mV. Cyclic voltammetry (CV) curves were recorded on an AUTOLABPGSTAT302N electrochemical workstation at a scanning rate of 0.1 mV

s⁻¹. The direct current (DC) polarization measurement was carried out to evaluate the electronic conductivity of materials using symmetric cells with the configurations of stainless-steel disk/Au/I-S@pPAN (or S@pPAN)/Au/stainless-steel disk. The prepared powder was pressed into pellet with a diameter of 13 mm, and the gold spraying on pellet was conducted to improve the interfacial contact between stainless-steel disk and pellet. The four-probe measurement was carried out on KEITHLEY 2450 to further explore the electronic conductivity of the prepared materials. As the electrical resistivity of pure S@pPAN (or I-S@pPAN) was out of the test range of KEITHLEY 2450, the S@pPAN (or I-S@pPAN):Super P pellets with a ratio of 8:1 were measured to evaluate the conductivity of the whole positive electrode. The equilibrium potentials of the batteries were obtained by the galvanostatic intermittent titration (GITT) technique, which consists of a series of current pluses at 0.1C for 20 min, followed by a 2 h relaxation. The sodium ion coefficient (D_{Na^+}) was calculated by the equation 1:

$$D_{Na^+} = \frac{4}{\pi\tau} \left(\frac{m_B V_M}{M_B A} \right)^2 \left(\frac{\Delta E_s}{\Delta E_t} \right)^2 \quad (1)$$

Here, the τ , m_B , V_M , M_B , A were duration of the current pulse (s), the mass, the molar volume (cm³ mol⁻¹), molecular weight (g mol⁻¹) and the electrode/electrolyte contacting area (cm²), respectively. ΔE_s was the steady-state voltage change and ΔE_t was the voltage change during the constant current pulse.

1.3 Material characterization

The morphology and elemental mapping of the as-prepared materials were investigated by field-emission scanning electron microscopy (FESEM, FEI Helios Nanolab 600i). The sulfur elemental contents of the materials were determined by means of elemental analyzer based on TurboFlashTM Combustion Technology (CHNS, EA 3000, Elementar). The X-ray diffraction (XRD) patterns were collected by a Netherlands' PANalytical X'pert power diffractometer with Cu K α radiation ($\lambda=1.54$ Å). The Raman spectra were obtained using a Horiba Jobin Yvon Labram-HR800 micro-Raman system with a 532 nm YAG laser excitation. X-ray photoelectron spectroscopy (XPS) measurements were carried out with a Thermo Fisher Scientific

ESCALAB 250XI spectrometer using a monochromic Al K α source (1486.6 eV). Fourier transform infrared spectra were taken using a Bruker Vertex 70 FTIR spectrometer.

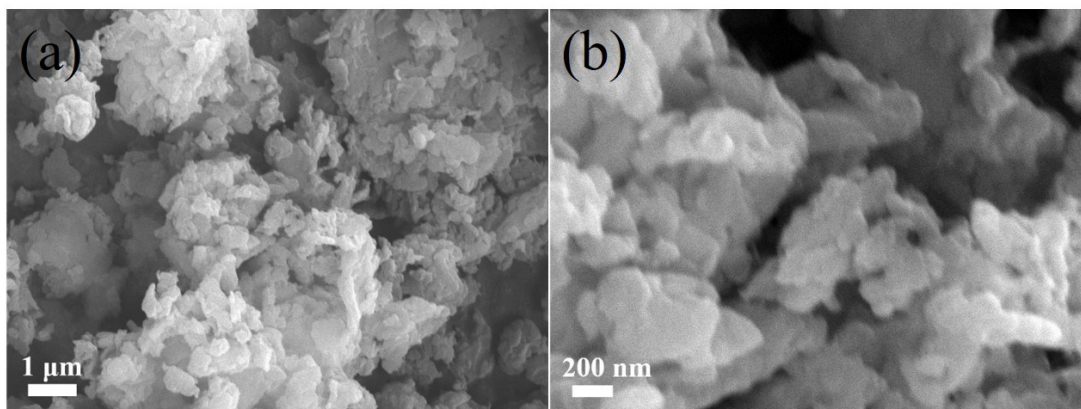


Figure S1. The SEM images of I-S@pPAN with different magnification, scale bars: 1 μm (a); 200 nm (b).

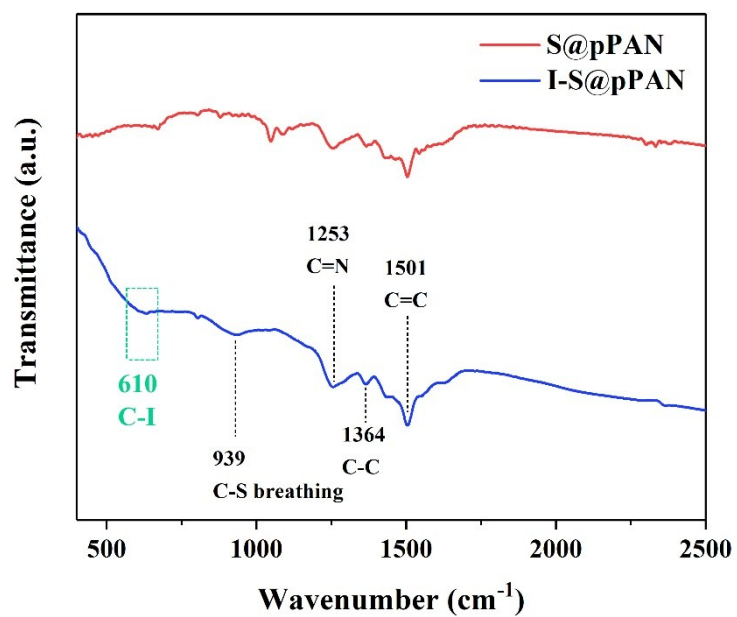


Figure S2. FT-IR spectra of S@pPAN and I-S@pPAN.

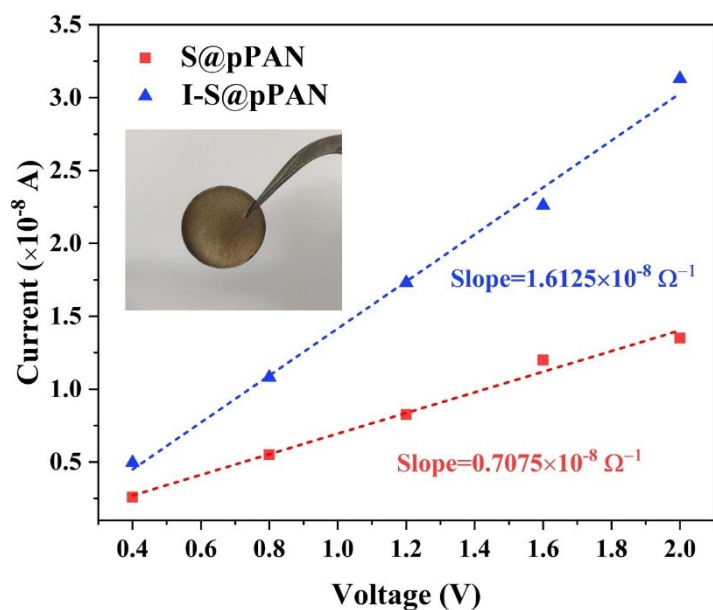


Figure S3. Equilibrium currents of the S@pPAN and I-S@pPAN at various voltages using DC polarization method.

Table S1. Electric conductivity of S@pPAN and I-S@pPAN measured by DC polarization method and calculated according to the following equation ($\sigma_e = (I \cdot L) / (U \cdot S)$).

Sample	Resistance ($\times 10^{-8} \Omega$)	Thickness of pellet (L, cm)	Area of pellet (S, cm^2)	Electric conductivity (σ_e , S cm^{-1})
S@pPAN	1.413	0.0575	1.326	3.07×10^{-10}
I-S@pPAN	0.617	0.0485	1.326	5.90×10^{-10}

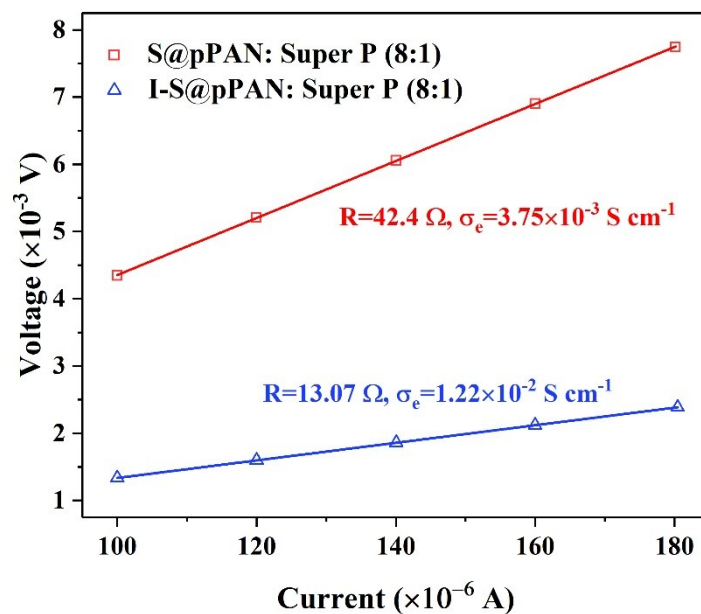


Figure S4. Equilibrium voltages of the S@pPAN (or I-S@pPAN): Super P (8: 1) composites at various currents using four-probe method.

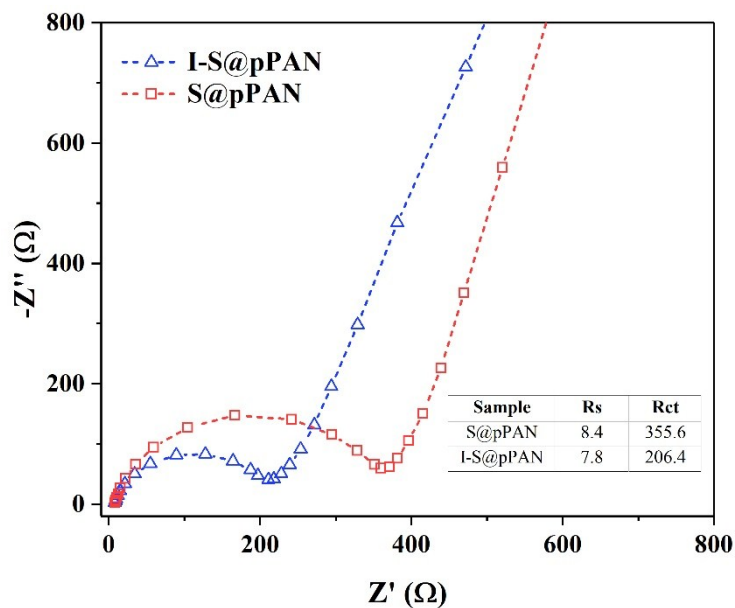


Figure S5. Nyquist plots of the cells with S@pPAN and I-S@pPAN cathodes.

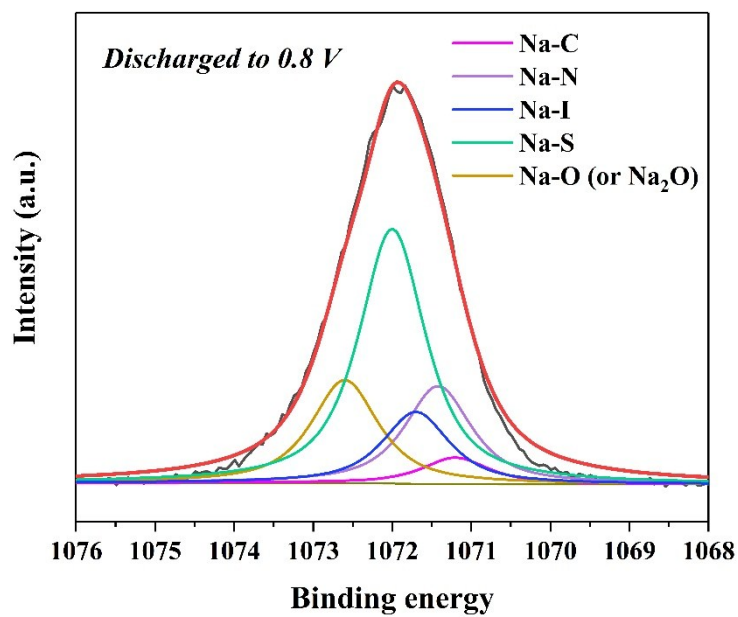


Figure S6. High-resolution Na 1s spectra of I-S@pPAN at initial fully discharged stage.

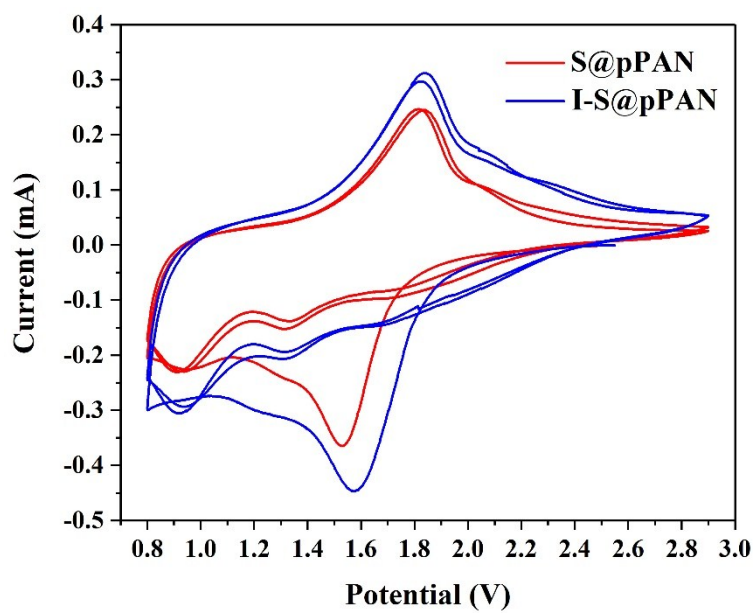


Figure S7. CV curves of S@pPAN and I-S@pPAN in RT-K/S battery.

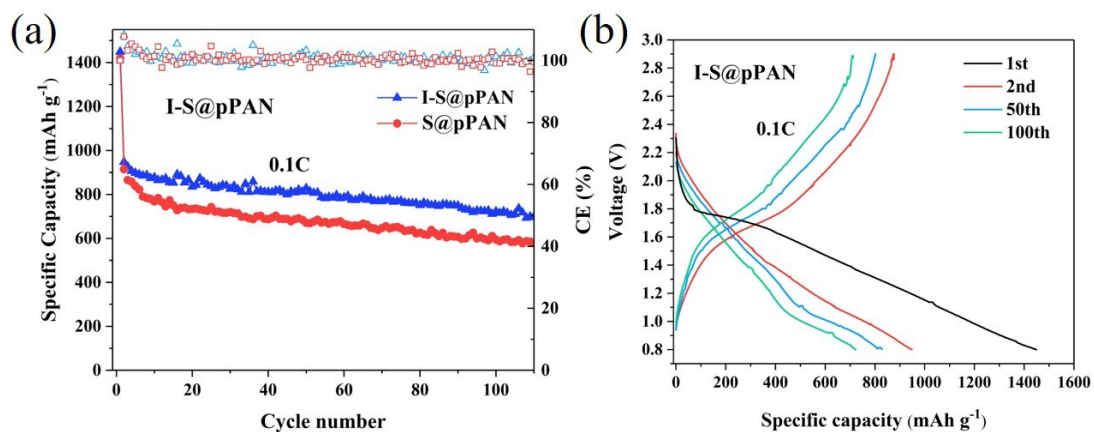


Figure S8. (a) Cycling performance of different cathodes for RT-K/S battery at 0.1C for 110 cycles, (b) The corresponding discharge/charge curves for RT-K/S battery of I-S@pPAN at 0.1C.

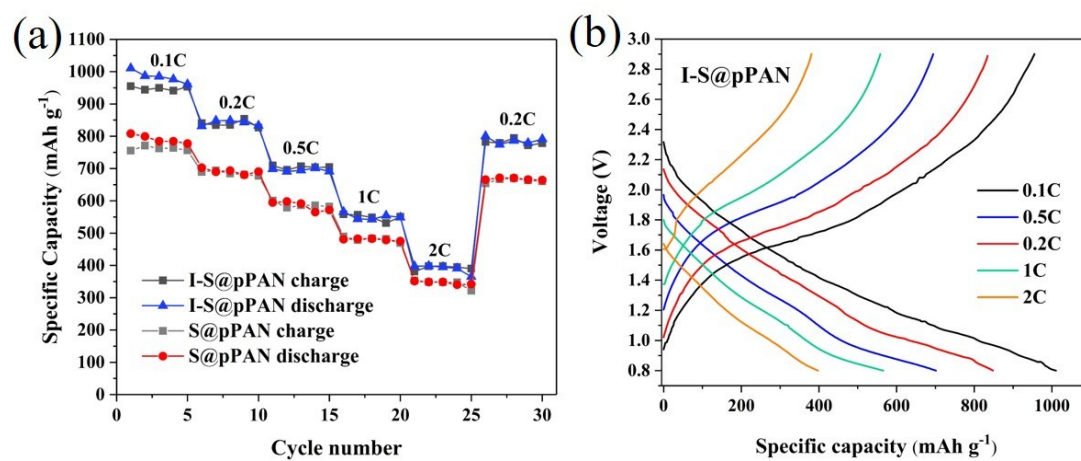


Figure S9. (a) Rate performance of cathodes for RT-K/S battery with rates ranging from 0.1C to 2C, (b) Representative voltage profiles of the I-S@pPAN cathode at various C rate.

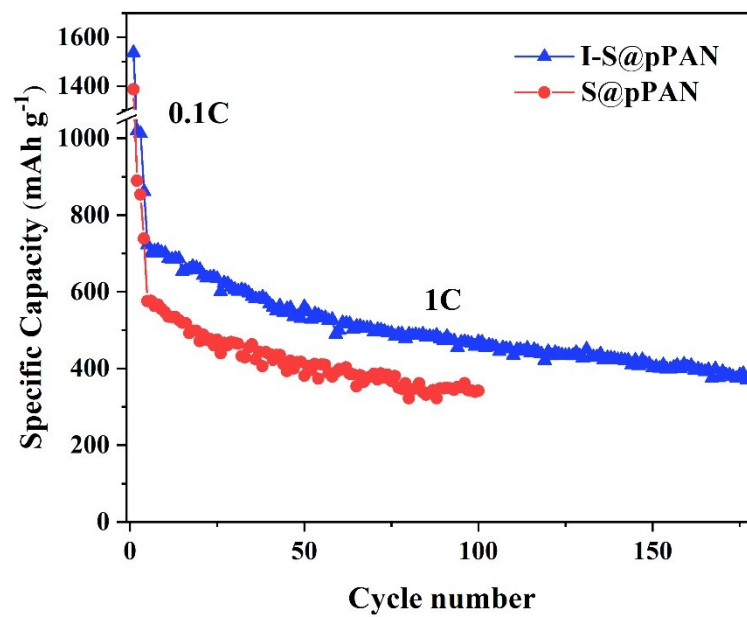


Figure S10. Long-term cycling stability of electrodes for RT-K/S battery at 1C over 500 cycles.